

Dark photon physics in SBND

Final report prepared for the Summer School held at Fermilab from July until October 2023

Gaetano Fricano, Supraja Balasubramanian, Vishvas Pandey

October 23, 2023

Abstract

This scientific report explores the potential for detecting dark photons within the Short-Baseline Neutrino Detector (SBND) at Fermilab. The study focuses on dark photon masses of 0.2 GeV, 0.3 GeV, and 0.4 GeV, and seeks to distinguish dark photon decay events from background events generated by neutrino interactions with argon nuclei. The event selection methods involving electron-positron pairs are explained, and an energy selection is performed on the events. The results indicate that dark photon decay events tend to be more energetic than background events, allowing for effective event selection. Additionally, the presence of hadrons in the background events is analyzed, revealing the potential to reduce background contamination significantly. Overall, this research offers valuable insights into detecting sub-GeV dark matter particles and developing event selection strategies in neutrino experiments.

1 Short Baseline Neutrino

The Short-Baseline Neutrino (SBN) program, located at Fermilab, comprises three Liquid Argon Time Projection Chamber (LArTPC) neutrino detectors positioned along the path of the Booster Neutrino Beam (BNB). The primary objective of this program is to perform precise measurements of neutrino oscillations, ultimately aiming to enhance our understanding of this phenomenon and to either confirm or refute the existence of sterile neutrinos.

Other than this the features of this program pave the

way for the study of physics beyond the Standard Model.

1.1 Booster neutrino Beam

The Booster Neutrino Beam (BNB) is utilized to produce a beam of neutrinos, and potentially in this case, Dark Matter (DM) particles, which is directed towards SBND. This beam is generated by extracting protons with a kinetic energy of 8 GeV from the Booster synchrotron accelerator and directing them onto a beryllium target. The proton extraction into the BNB is organized with a spill structure consisting of $4 \cdot 10^{12}$ protons distributed across 81 Gaussian bunches, which are spread over a spill duration of 1.6 microseconds. Each of these Gaussian bunches is approximately 2 nanoseconds wide and separated by 19 nanoseconds. This configuration results in the production of a beam comprising secondary particles, notably pions, which subsequently decay into neutrinos within the 50-meter-long decay pipe filled with air. This decay process occurs downstream of the target and magnetic focusing horn

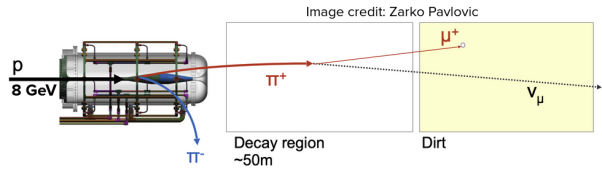


Figure 1: Booster neutrino beam craction

The operation of the BNB generates a substantial flux of neutrinos, especially at SBND, owing to its

short baseline.

Additionally, the magnetic focusing capabilities allow for operation in both neutrino and antineutrino modes. Here there is a typical flux in SBND

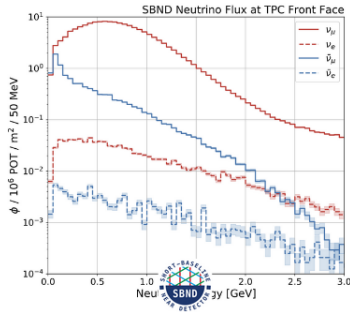


Figure 2: Neutrino flux at SBND

1.2 LArTPC

In recent years, the Liquid Argon Time Projection Chamber (LArTPC) has emerged as the preferred detector technology for numerous neutrino physics experiments. Its ability to provide high-resolution 3D images of particle interactions, scalability, and precise calorimetry make it the perfect choice for applications in the search for Dark Matter (DM) as well. The following scheme shows the typical LArTPC setup

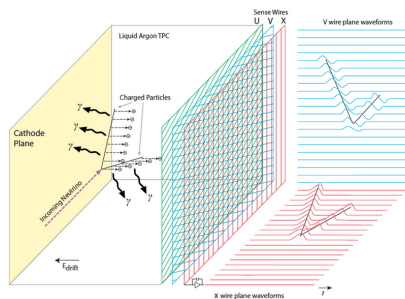


Figure 4: Time Projection Chamber

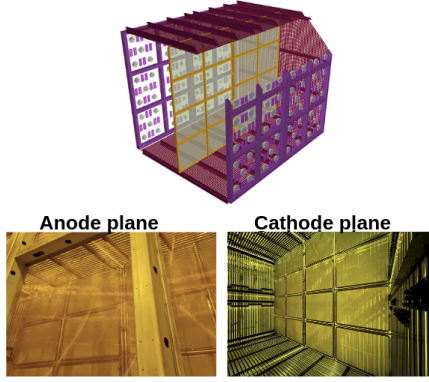
A LArTPC comprises a substantial volume of purified liquid Argon housed within a cryostat, maintaining

the Argon at a constant temperature. An unvarying electric field is established across the active volume through an anode and cathode plane. When charged particles traverse the liquid Argon, they generate a trail of ionization electrons. These electrons are accelerated towards the anode plane due to the applied electric field. Argon’s chemically inert properties allow ionization electrons to drift over significant distances within the detector. The anode consists of three wire planes: two induction planes and one collection plane. These wire planes record the position of the particle track when the ionization electrons induce electrical signals on the wires. Electrons pass through the first two induction planes before being collected on the third wire plane.

A valuable feature of LArTPCs is that the wire planes can measure the rate of energy loss $\frac{dE}{dx}$ of a particle track by examining the total charge collected in each wire hit. This capability can effectively discriminate between signal and background events. The wire signal readouts alone produce a 2D image of the particle event. The third dimension is determined by the charge drift time, which is calculated using scintillation light to establish a trigger for when an event takes place. A substantial portion of the energy in a LArTPC event is emitted as scintillation light. Under zero electric field conditions, liquid Argon produces approximately 40,000 photons per MeV of energy deposited in the vacuum ultraviolet (VUV) frequency range. Scintillation light is detected by photon detectors, such as photomultiplier tubes, positioned behind the anode plane.

Short Baseline Near Detector

The Short Baseline Near Detector (**SBND**) is the closest detector to the target of the three-detector complex. It is a Liquid Argon Time Projection Chamber (LArTPC) at 110m from the BNB target and with a 112-ton active volume of liquid Argon. The TPC dimensions for SBND are 4 meters by the transverse plane and extend for 5 meters along the beam axis. SBND comprises two drift volumes that are separated by two central cathode plane arrays (CPAs), with each drift volume being bounded at either end by two anode plane arrays (APAs).

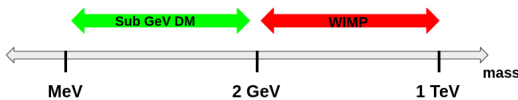


Each APA is composed of three wire planes, with the two induction planes oriented at angles of ± 60 degrees relative to the vertical collection plane. Each of these wire planes is equipped with wires spaced 3 millimeters apart.

2 Theoretical background: Sub-GeV dark matter

Despite numerous experiments aimed at detecting WIMP particles, nothing has been found yet that can confirm or refute their existence. For this reason, in recent years, the idea of searching for new candidates for dark matter with sub-GeV masses has gained momentum.

However, as shown before, it is not possible to search for WIMPs with these characteristics due to the Lee-Weinberg limit.



One way to evade this limit is to hypothesize that the particles being sought do not interact through weak interaction, as was assumed for WIMPs, but rather through a new interaction.

From a theoretical standpoint, this is equivalent to postulating the existence of a new gauge field with

its corresponding mediator boson.

In the pursuit of considering sub-GeV dark matter as a thermal relic, it is necessary to hypothesize that dark matter and the Standard Model interact through the new interaction.

Equally significant, there would be no hope of detection if there were no interactions with the Standard Model.

To this end, we refer to the concept of **portal** between the dark sector and the Standard Model. There can be various types of portals distinguished by their spin properties. The focus of this project lies on the vector portal.

2.1 Vector portal: Dark Photon

It is usual to refer to the mediator boson as the dark photon, which is a particle with spin 1. In this simple scenario, the gauge symmetry employed is $U(1)'$, and we are able to apply the Higgs mechanism, resulting in a non-zero mass associated with the dark photon. A crucial aspect to consider is the requirement that the dark photon mediates interactions between dark matter and the Standard Model, as mentioned earlier. To incorporate this requirement into the theoretical model, we introduce the concept of a **kinetically mixing parameter** ϵ . This parameter allows the dark photon to transform into a mediator of the Standard Model, giving rise to Standard Model particles.

In further detail, for the dark photon to interact with the Standard Model, it needs to interact with hypercharge. However, given our focus on energies that are not particularly high, we can assume that the dark photon interacts exclusively with $U(1)_{em}$, that is, it transforms into a photon depending on the mixing parameter. This allows us to construct a Lagrangian

$$L = \frac{1}{4}F_{\mu\nu}F^{\mu\nu} - \frac{1}{4}F'_{\mu\nu}F'^{\mu\nu} + \frac{\epsilon}{2}F_{\mu\nu}F'^{\mu\nu} + eA_{\mu}J_{em}^{\mu} + d_D V_{\mu}J_D^{\mu} + \frac{1}{2}m_V^2 V_{\mu}V^{\mu}$$

where $J_D^{\mu} = \bar{\chi}\gamma^{\mu}\chi$.

It is possible also to do a field redefinition in order to remove the mixing term, taking care not add any

mass term for the standard model photon

$$\begin{aligned} V &\longrightarrow V \\ A &\longrightarrow A + \epsilon V \end{aligned}$$

consequently one obtain

$$eA_\mu J_{em}^\mu \longrightarrow eA_\mu J_{em}^\mu + \boxed{\epsilon e V_\mu J_{em}^\mu}$$

The highlighted term indicates that each electrically charged particle in the Standard Model possesses a dark millicharge. This has significant implications, as in all cases involving electric charge, we can trace back to a dark photon, both in decay and production channels.

2.2 Why are we interested in SubGeV dark matter

Among the most plausible candidates for dark matter particles are WIMP particles.

The theoretical model suggests that these particles formed following the Big Bang during the hottest and densest phases in the history of the universe. Due to the high energies available during this period, WIMP particles are hypothesized to possess a high mass ranging from GeV to TeV. Later, as a consequence of the universe's expansion and subsequent cooling, WIMPs would have cooled down, reaching thermal equilibrium with the standard model and interacting with it through the weak interaction.

In doing so, they would have significantly reduced their chances of decaying. This model is known as the **thermal relic model**.

One of the notable strengths of this theory is referred to as the 'WIMP's miracle.' Essentially, to ensure the robust thermal equilibrium achieved, it is necessary for the cross-section of WIMPs to be such that it doesn't create an overabundance that would disrupt this equilibrium. What is truly remarkable is that, within the assumptions of the model, this condition is met.

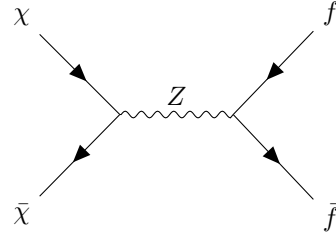
Closely tied to the cross-section is the mass, and in particular, the upper and lower limits constitute a key point of the theory. It is worth noting that

$$\Omega \sim \frac{1}{\sigma}$$



As for the upper limit, it's understood that we cannot have excessively large masses, as this would result in an extremely low cross-section, making it impossible to defeat enough dark matter to satisfy the relic abundance.

As for the lower limit, this is well-known as the Lee-Weinberg limit. To understand its origin, let's consider the annihilation of two WIMP particles, which we denote as χ , through the Z boson, resulting in two Standard Model particles denoted as f



The lagrangian that allows us to describe this process is like

$$L \sim G_F (\bar{\chi} \gamma^\mu \chi) (\bar{f} \gamma^\mu f)$$

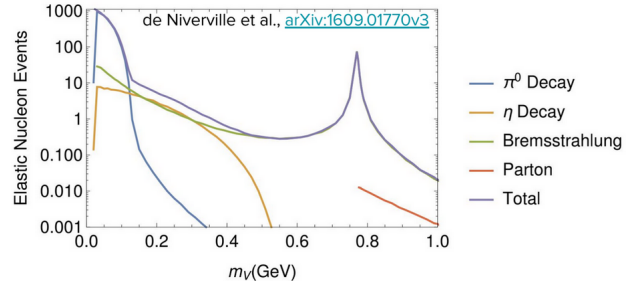
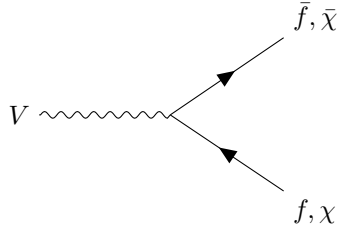
when calculating the cross-section for this process

$$\sigma \sim \frac{G_F^2 m_\chi^2}{\pi} \sim 1pb \left(\frac{m_\chi}{5GeV} \right)^2$$

As can be seen, it is normalized to 1 pb, which is the typical cross-section for weak interaction. If we now decrease the mass of the WIMP particle below 5 GeV, the cross-section decreases, and according to the relationship with abundance, it would increase, contradicting the thermal relic model.

2.3 Dark photon decay

Taking into account the theory one can calculate all the useful parameters of the decay. The decays that can occur are as follows, where, as usual, we refer to particles of the Standard Model with f



Below is a graph of the branching rates as a function of the mass of the dark photon we are considering

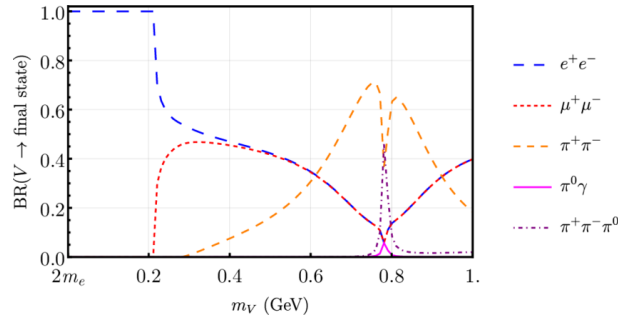


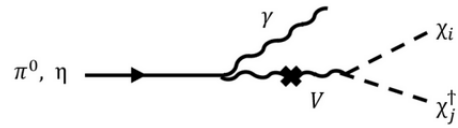
Figure 5: Decay channels branching ratio

2.4 Dark photon production in SBND

An essential aspect to consider in the context of detecting the dark photon is the issue of its production, particularly why it can be detected in SBND. As previously shown, in the process of generating the neutrino beam within the decay pipe, mesons in all charge states are produced due to proton scattering with the beryllium target. Below is a graph illustrating the production channels that can occur with these particles as a function of the dark photon's mass

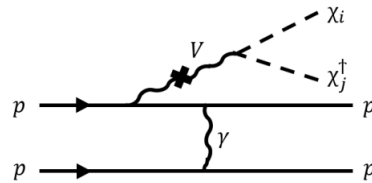
As it shows, using neutrino experiment we could detect dark photons with mass less than $\sim 0.6 GeV$.

2.4.1 π^0 and η decay



In this decay, one of the two photons that come from the π_0 or η decay is supposed to become a dark photon that subsequently decays into two dark matter particles.

2.4.2 Proton bremsstrahlung



In this decay, the photon emitted by one of the two protons is supposed to become a dark photon that subsequently decays into two dark matter particles.

2.4.3 Charged meson decay

In more recent times, another decay channel has also been hypothesized involving charged mesons, which are also produced during the neutrino beam production. Once one of these channels decays take place,

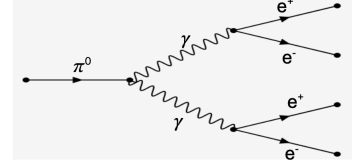
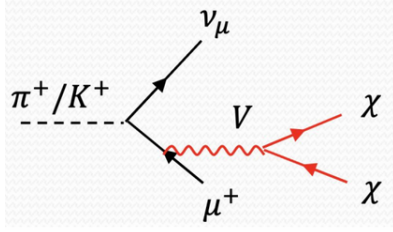


Figure 6: π_0 decay inside SBND

the dark matter particles can propagate through the decay pipe, and once get the detector they could decay.

When one of these decays takes place, one of the two produced particles can join the detector

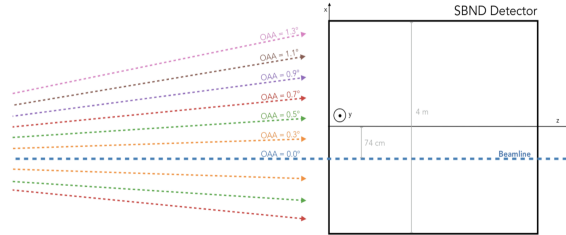


Figure 7: PRISM measures

3 Analysis

As shown in the preceding sections, it is evident that, according to the model presented, there are possibilities for detecting dark photon decay events within the SBND (Short-Baseline Neutrino Detector). As depicted in Figure 5, there are multiple decay possibilities. In this study, we have focused on dark photon masses of 0.2 GeV, 0.3 GeV, and 0.4 GeV. This implies that the dominant decay channel is the one leading to electron-positron pairs. Of course, for a comprehensive analysis, all potential decay channels must be considered. However, it is certainly the most challenging to characterize electrons and positrons.

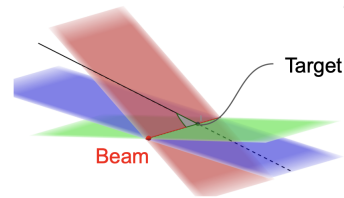
3.1 Background source

The primary source of background that needs to be considered will be the π_0 mesons produced in neutral current interactions of neutrinos with argon. Taking these considerations into account, the concept is that these events should exhibit a significant concentration in the vicinity of the incident beam, as has already been analyzed in prior studies of neutrino PRISM measurements

The idea is to investigate the PRISM measurements anticipated from simulations of dark photon decay and attempt to differentiate between the expected signal and the background.

3.2 Dark photon PRISM measures

To better understand the meaning of "PRISM measures", here is a graphical representation



Below are the comparison graphs of PRISM measurements between dark photon decay simulations and neutrino background measurements

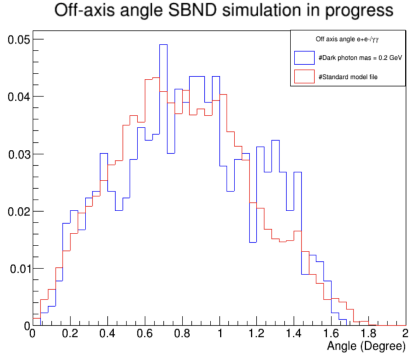


Figure 8: 0.2 GeV compare

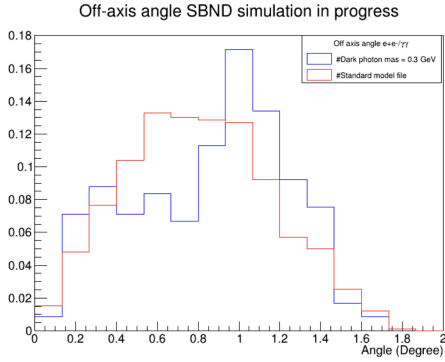


Figure 9: 0.3 GeV compare

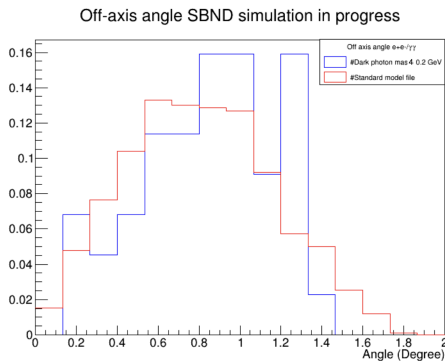


Figure 10: 0.4 GeV compare

As it is evident in all cases, the measurements exhibit significant overlap, making it challenging to

perform a selection. This implies a need to evaluate other quantities related to the two simulation datasets, allowing for the application of new criteria to the PRISM measurements to make them distinguishable.

3.3 Event selection cuts

The primary quantity chosen for the selection process is the energy of the electron-positron pair for both simulation datasets. However, before proceeding with the selection, it is important to clarify the method used to identify pairs from the two simulation datasets. Essentially, what was done was to combine a spatial condition on the order of 1 cm with the fiducial volume condition. In practice, once an electron-positron pair was found within the fiducial volume if the two particles in question originated within a distance of less than 1 cm, they were considered an electron-positron pair. To determine the correctness of this method, two specific quantities were assessed:

- The invariant mass.
- The norm of vectorial difference.

3.3.1 Norm of vectorial difference

To assess the correctness of the 1 cm spatial condition, it was decided to estimate the distance between the origins of the two particles by calculating the difference between the vectors that identified them. As can be observed in the following chart, all the identified particles have origins at a distance of less than 1 cm

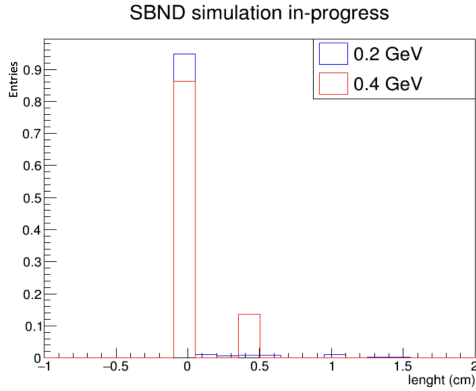


Figure 11: Norm of vectorial difference for 0.2 GeV and 0.4 GeV files

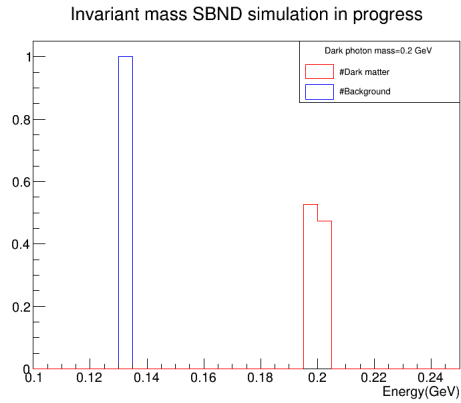


Figure 12: Invariant mass comparison between dark photon simulation files and background

In the figure it is possible to see the different invariant masses of the two processes and as we can see the findings show a total agreement with the well-known mass of the π_0 and of the simulated dark photon.

3.3.2 Invariant mass

To do an event selector able to distinguish between the dark photon decay and the π_0 decay, it is surely a good idea to evaluate the invariant mass of the two processes. The invariant mass is a characteristic of the system's total energy and momentum that is the same in all frames of reference related by Lorentz transformations, it tells us about the mother particle of the e^+e^- and $\gamma\gamma$ event.

For a two-particle system, the invariant mass can be computed with the following expression

$$M = \sqrt{(E_1^2 + E_2^2) - \|\vec{p}_1 + \vec{p}_2\|^2}$$

3.4 Energy selection

Following the procedure explained before, all electron-positron pairs within the fiducial volume were identified for both datasets. Subsequently, an analysis of the energies of the individual components of the pairs and their respective comparison was carried out. Below are the comparative data

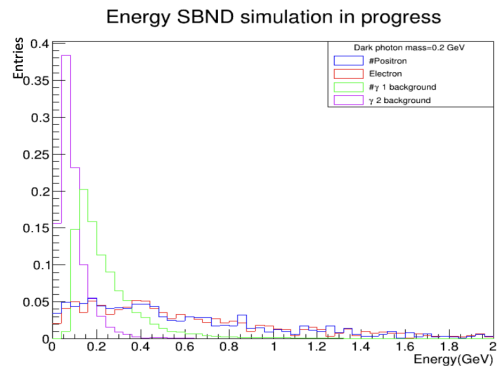


Figure 13: 0.2 GeV energy compare

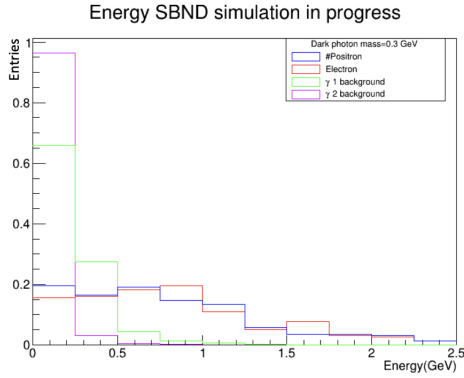


Figure 14: 0.3 GeV energy compare

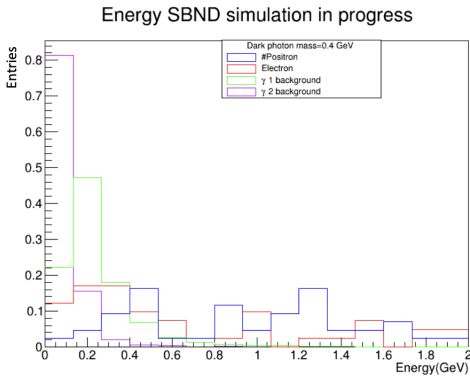


Figure 15: 0.4 GeV energy compare

Findings show that the electron-positron pairs originating with the dark photon decay are more energetic than the electron-positron pairs originating by neutral current neutrino-Argon interaction. This allows us to perform a selection that will subsequently be applied to PRISM measurements. In addition to an initial graphical analysis, to make a selection, one must strive to maximize the number of dark photon decay events while minimizing the number of background events. In this regard, we introduce the fol-

lowing efficiency parameters

$$\text{Efficiency}_{\text{signal}} = \frac{\text{Signal events selected}}{\text{Total events}}$$

$$\text{Efficiency}_{\text{background}} = \frac{\text{Background events selected}}{\text{Total events}}$$

The following plots illustrate these quantities as a function of the energy value at which it is deemed most appropriate to apply the cut. The red circle indicates the values that appear to meet the criteria for maximizing and minimizing the two efficiencies.

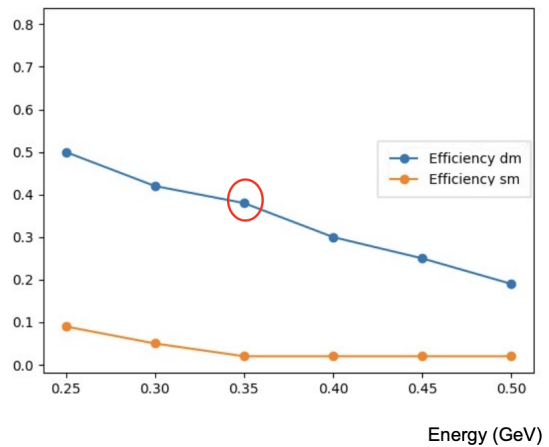


Figure 16: 0.2 GeV efficiency plot

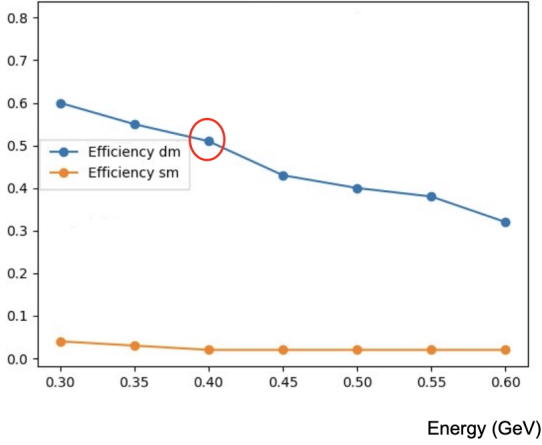


Figure 17: 0.3 GeV efficiency plot

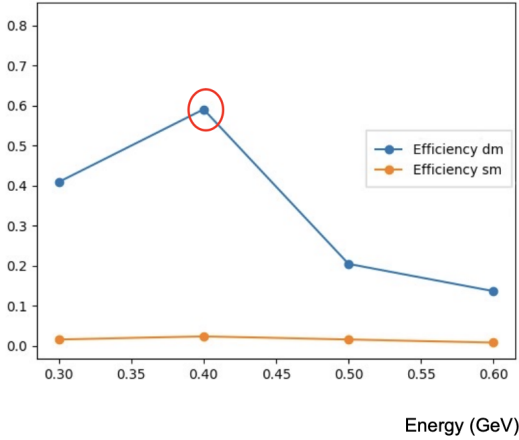


Figure 18: 0.4 GeV efficiency plot

3.5 Hadron search

Certainly, besides energy, there are other quantities that can be evaluated for event selection. Here, The focus is the search for hadrons in events that produce electron-positron pairs from the background files. This choice is justified by the fact that when neutrinos interact with argon nuclei, if they are energetic enough, baryonic resonances can be created within the nuclei, which will decay, releasing hadrons in addition to the other discussed products.

Of course, this phenomenon does not occur in dark photon decay events, so this can be another selection parameter to apply. In this project, a complete selection like the one done for energy was not achieved; however, the number of events containing a certain number of hadrons was examined

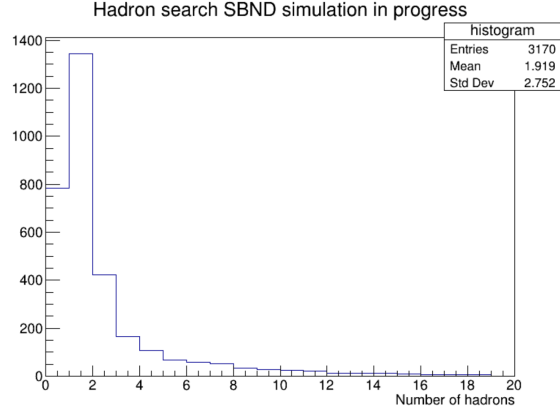


Figure 19: Number of events as a function of the number of hadrons

From the plot, we can observe that the majority of background events feature only one hadron, and this is typical of the SBND configuration. In general, there is a high number of events with one or more hadrons; in this particular case, approximately one-quarter of the events do not have any hadrons. This result is significant as it effectively eliminates a substantial number of background events.

3.6 About the event display

Certainly, these events can be visualized; however, if the angles between electrons and positrons are too small, this may become challenging. In anticipation of future work involving event display, it has been decided to display the opening angles between electrons and positrons

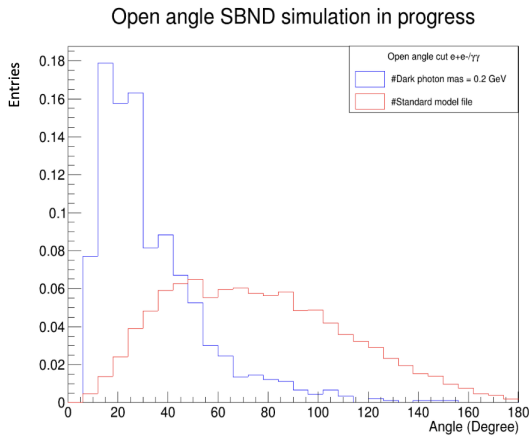


Figure 20: 0.2 GeV open angle

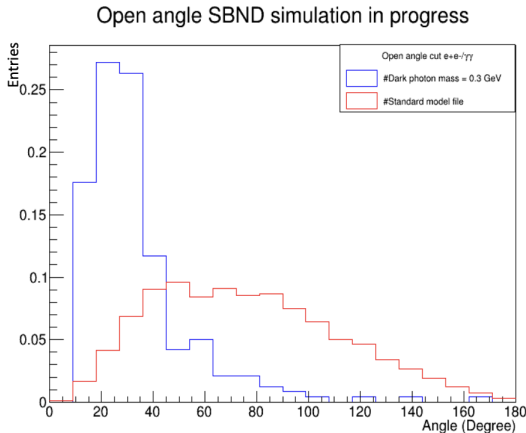


Figure 21: 0.3 GeV open angle

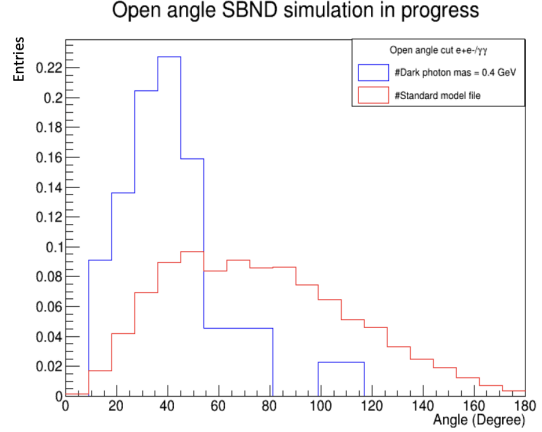


Figure 22: 0.4 GeV open angle

In these plots, the opening angle between the photons produced in the decay of π_0 is also included to determine whether the vertices of background events can be well distinguished or not. As we can see, concerning the dark photon decay events, the angles in this initial analysis appear to be sufficiently large to enable the proper visualization of events. Additionally, we can observe that, on average, these angles increase with the increasing mass of the dark photon.

4 Conclusion and next steps

In this project, we have initiated work on event selection with the aim of distinguishing potential dark photon decay events within SBND. Specifically, we intend to utilize PRISM measurements, which, however, exhibit substantial overlap with background measurements. To address this challenge, we have commenced a study of the properties of the two simulation files, starting with the energy of the electron-positron pairs. This study has revealed a practical opportunity to implement cuts on the measurements. Additionally, we have initiated an investigation into the presence of hadrons in background events, which will enable further refinement of the selection process. As the next steps in this study, we propose to acquire a larger dataset to facilitate more precise analyses,

examine the invariant mass of processes that were previously inaccessible due to the limited availability of simulation files, and ultimately apply these selection criteria to the PRISM measurements.

5 Acknowledgment

For this work, I would like to express my gratitude, first and foremost, to my supervisors, Supraja Balasubramanian and Vishvas Pandey. Despite their busy schedules, they have always been available for any clarification and advice. I genuinely hope to have the opportunity to work with them again in the near future. I would also like to thank the project organizers who provided me with the opportunity to gain this valuable experience. This journey has been of immense importance for my scientific and personal growth. I am truly grateful for their support.

6 Bibliography

- Light Dark Matter in SBND, Supraja Balasubramanian
- Searching for Dark Matter in Neutrino detectors, Ciaran Hasnip
- SBND-PRISM: Sampling Multiple, Off-Axis Fluxes with the Same Detector. MARCO DEL TUTTO
- de Niverville et al., arXiv:1609.01770v3